Ecological Indicators 133 (2021) 108405

Contents lists available at ScienceDirect

Ecological Indicators

journal homepage: www.elsevier.com/locate/ecolind

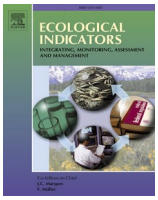

Original Articles

# Marine pollen records provide perspective on coastal wetlands through Quaternary sea-level changes

Zhongjing Cheng [a], Chengyu Weng [a,*], Stephan Steinke [b], Mahyar Mohtadi [c]

[a] State Key Laboratory of Marine Geology, Tongji University, Shanghai 200092, China
[b] Department of Geological Oceanography and State Key Laboratory of Marine Environmental Science, Xiamen University, Xiamen 361005, China
[c] MARUM–Center for Marine Environmental Sciences, University of Bremen, Bremen D28359, Germany

ARTICLE INFO

*Keywords:*
Ecological sustainability
Glacial cycle
Palaeoecology
South China Sea
Salt marsh
Vegetation succession

ABSTRACT

The response of coastal wetlands to future sea-level rise remains uncertain. Palaeoecological data are essential to constrain the still conflicting ecological models. However, obtaining detailed palaeo-coastal stratigraphic records before Holocene is often difficult due to repeated Quaternary marine transgression-regressions. Here we utilize pollen data from a deep-sea sedimentary archive in northern South China Sea to explore the historical behavior of coastal wetlands at a large river estuary over the last 140-kyr. A recurrent wetland (Cyperaceae)-pioneer species (*Selaginella*)-zonal forest (*Pinus*) succession throughout the last glacial-interglacial cycle implies a coastal salt marsh origin of the Cyperaceae pollen. Comparing with global sea-level reconstructions, the increases in Cyperaceae pollen abundance, and hence the expansions of coastal salt marsh, were found to be closely linked with rapid large-scale sea-level rises. This finding indicates a resilience of coastal wetlands to future sea-level rise, and highlights the probable importance of conventionally ignored horizontal adaptability in long-term survival of coastal wetlands. Overall, marine pollen records provide an opportunity to supplement existing palaeoecological observations of coastal wetlands during the Quaternary.

## 1. Introduction

Coastal wetlands are among the most valuable ecosystems on Earth. Marshes and mangroves sequestrate carbon (Duarte et al., 2013), protect coasts from storms (Möller et al., 2014), support commercial fisheries (Aburto-Oropeza et al., 2008), and maintain biodiversity (Millennium Ecosystem Assessment, 2005). Yet uncertainty persists about their response to future sea-level change. Early static landscape models predict that up to 90% of present coastal wetlands will be submerged by the end of this century, with sea-level rise rates of less than 8 mm/yr (Nicholls et al., 2007; Craft et al., 2009; Nicholls & Cazenave, 2010), whereas more recent dynamic models suggest that, through ecogeomorphic feedbacks between increased inundation and enhanced vertical accretion, coastal wetlands will be resistant to sea-level rise rates of 10–50 mm/yr (Kirwan et al., 2010; Kirwan & Megonigal, 2013; Kirwan et al., 2016a), exceeding the worst scenarios considered by the IPCC (8–23 mm/yr in RCP 8.5, Church et al., 2013).

Palaeoecological data not merely provide empirical tests of existing models, but also may pave the way for further ecological researches by demonstrating ecosystem dynamics over timespans much longer than those of modern observations and experiments (Brewer et al., 2012; Barnosky et al., 2017). For instance, according to Holocene coastal stratigraphic records, tidal marshes in Great Britain (Horton et al., 2018), Mississippi Delta (Törnqvist et al., 2020) and Florida (Parkinson et al., 2015) had converted to open water within decades when sea-level rise rates were > 6–8 mm/yr, although vertical accretion of the marshes did increase (Rogers et al., 2019). It has therefore been argued that the dynamic models, based largely on ecological observations over decades or less, have failed to capture key processes and stochastic nature of wetland evolution at millennial or longer scale, such as sediment compaction, extreme climatic influences and catastrophic ecosystem shifts, and underestimated the vulnerability of coastal wetlands to future sea-level rise (Fagherazzi et al., 2012; Parkinson et al., 2016; Törnqvist et al., 2020).

Going back before the Holocene, the Quaternary includes a wider variety of sea-level change scenarios (Siddall et al., 2003; Grant et al., 2012) to explore more detailed evolutionary dynamics of coastal wetlands. However, lots of earlier coastal sedimentary sequences have been buried and/or eroded during large-scale cycles of marine transgression-regression, impeding direct investigations of wetland sustainability

* Corresponding author.
*E-mail address:* weng@tongji.edu.cn (C. Weng).

https://doi.org/10.1016/j.ecolind.2021.108405
Received 30 September 2021; Received in revised form 8 November 2021; Accepted 20 November 2021
Available online 9 December 2021

through large numbers of stratigraphic records across the palaeo-coastal region (like Horton et al., 2018; Törnqvist et al., 2020). Fortunately, a few studies hint that coastal wetland vegetation might have left distinct pollen signature in offshore sediments. For instance, a recurrent temporal succession in the pollen record of marine core MD03-2622, Cariaco Basin, during MIS 3, starts with Chenopodiaceae (hypersaline-tolerant), followed by Cyperaceae, Poaceae and *Rhizophora* (wetland plants), subsequently by *Selaginella* (likely pioneer species), ends into the zonal forest species (González & Dupont, 2009; Fig. S1). Its resemblance to the spatial pattern of modern plant community along coastal environmental gradients (from intertidal to terrestrial environment, Fig. S2) suggests a potential to evaluate the behaviors of coastal wetlands through variations of indicator pollen in marine archives, and then the ecological observations of coastal wetlands could be greatly extended in space and time. Nevertheless, the taxonomic resolution is relatively low in palynological analysis. Poaceae and Cyperaceae, in particular, comprise a large number of species that occur in many other habitats besides coastal wetlands. It is also difficult to find modern analogue for some key taxa in the succession, such as *Selaginella*. The generality of this approach remains to be tested.

Here we present a 140-kyr long pollen record from the deep-sea sedimentary archive GeoB16602 in the South China Sea (SCS). Within a wider chronological frame, previously reported wetland succession (wetland plants–pioneer species–zonal forest) is replicated, validating the feasibility of indicator pollen (Cyperaceae in this case) from marine archives in tracking historical evolution of coastal wetlands. Differences between the successions of two sites (GeoB16602 and MD03-2622) imply that this approach may need to be adjusted according to biogeographical settings. Geomorphic conditions, as well as background noise, could cause the obscuring of wetland succession in offshore sediments. The implications for coastal wetland sustainability is also discussed by comparing our reconstructed wetland dynamics with global sea-level reconstructions.

## 2. Regional setting

The monsoonal climate of the northern SCS region is characterized by hot-humid summer and mild winter. The mean annual temperature of the region ranges from 20 °C to 27 °C with a latitudinal gradient. The mean annual precipitation is around 2200 mm, ~80% of which are brought in by the East Asian Summer monsoon between March and September (International Atomic Energy Agency, 2013). The Pearl River catchment represents an ecotone zone between the two major forest types of the region, i.e. subtropical evergreen broadleaved forest in the north and tropical monsoon forest in the south (Wu, 1980; Beck et al., 2018; Fig. S3). Mangroves are common along some tropical coasts of Hainan Island, but become much scattered to the north. For instance, salt marshes dominated by *Cyperus malaccensis* are more extensively distributed in the intertidal zone of Pearl River estuary (Zhao, 1996). The pollen deposits at southwestern part of northern SCS mainly indicate the historical vegetation evolution of the (palaeo-)Pearl River catchment area, without large provenance changes (Dai et al., 2014; Yu et al., 2017; Liu et al., 2017; Cheng et al., 2018).

## 3. Material and methods

The study site GeoB16602 (18.95°N, 113.71°E, water depth, 953 m) is located in the northwestern SCS (Fig. 1). A composite record was established by correlating the XRF data of two parallel cores (gravity core GeoB16602-4, 0.25–9.71 m and MeBo core GeoB16602-5, 9.59–17.07 m) recovered at the site during the 2012 RV SONNE cruise SO-221 "INVERS" (Mohtadi, 2012). The benthic foraminiferal $\delta^{18}O$ data was aligned with the globally stacked reference LR04 (Lisiecki and Raymo, 2005) using the program AnalySeries 2.0.8 (Paillard et al., 1996) in order to establish the long-term age model; the upper 5.62 m (0–36.8 ka) was constrained by 15 AMS $^{14}C$ dates using the Bacon

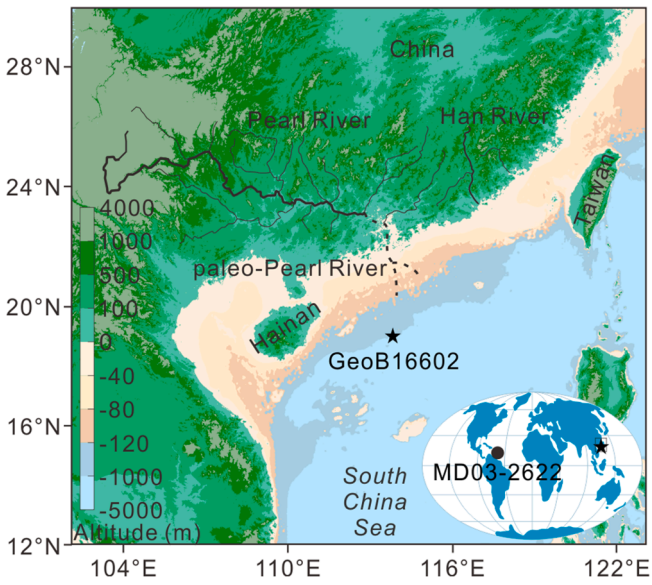


**Fig. 1.** Location of the study site GeoB16602 plotted on a topographic map. Also show a relevant marine pollen record from Criaco Basin on the global map inset (González and Dupont, 2009). Dashed lines indicate palaeo-River systems.

software (See Liu et al. (2017) for details about this part).

Pollen records spanning the interglacial intervals (0–30 ka and 95–140 ka) of GeoB16602 cores have been reported previously (Cheng et al., 2018). For this study, the last glacial interval (30–95 ka) was sampled to get a full view of the last glacial-interglacial cycle, with a 5–10 cm interval equivalent to an average temporal resolution of ~ 600 years. Pollen samples were processed via standard hydrochloric-hydrofluoric acid procedure (Fægri et al., 1989). A tablet containing 27,637 exotic *Lycopodium* grains was initially added to each sample for calculating the pollen concentrations (absolute abundances). The percentages (relative abundances, Fig. 2) of pollen and spore taxa were calculated on the pollen sum (>300 grains per sample) and spore sum (>100, on average 160 grains per sample) respectively in order to independently study the compositional changes of higher plant and fern communities. Principle components analysis (PCA) and cluster analysis on percentage data of all identified pollen and spore taxa were conducted using CANOCO (ter Braak & Smilauer, 1998) and Tilia (CONISS) software (Grimm, 1987), respectively.

## 4. Results

The variabilities in relative abundance of GeoB16602 pollen and spore taxa (Fig. 2) reveal two distinct evolution patterns at the tropical-subtropical flora ecotone of southern China:

1) the zonal forest exhibited a clear glacial-interglacial cycle. During the peak interglacials (MIS 1 and 5e), tropical components, here best expressed by the montane rainforest trees including *Dacrydium*, *Dacrycarpus*, *Podocarpus* and *Altingia* (15%-30% in total) and thermophilic ferns (such as *Dicranopteris and Cyathea*), are the most abundant. They give way step-wisely to temperate (e.g. *Pinus* and *Fagus*) and alpine trees (e.g. *Tsuga* and *Abies/Picea*), grasses (mainly Poaceae and Asteraceae), eurythermal ferns (e.g. Polypodiaceae) and some more cold-adapted lower plants (e.g. Hymenophyllaceae and *Anthoceros*) toward the Glacial Maximums (MIS 2 and 6). Component loadings for first principal components in PCA indicates a major biome shift, but not a species turnover, at MIS 3/4 boundary.

2) glacial/interglacial pattern are very ambiguous (similar peak values for MIS 2, 3 and 5) for Cyperaceae (from about 5–8% to 15%) and *Selaginella* (from 0 to 10%), in which millennial-scale fluctuations are persistent and more notable (Figs. 2 and 3). These fluctuations are

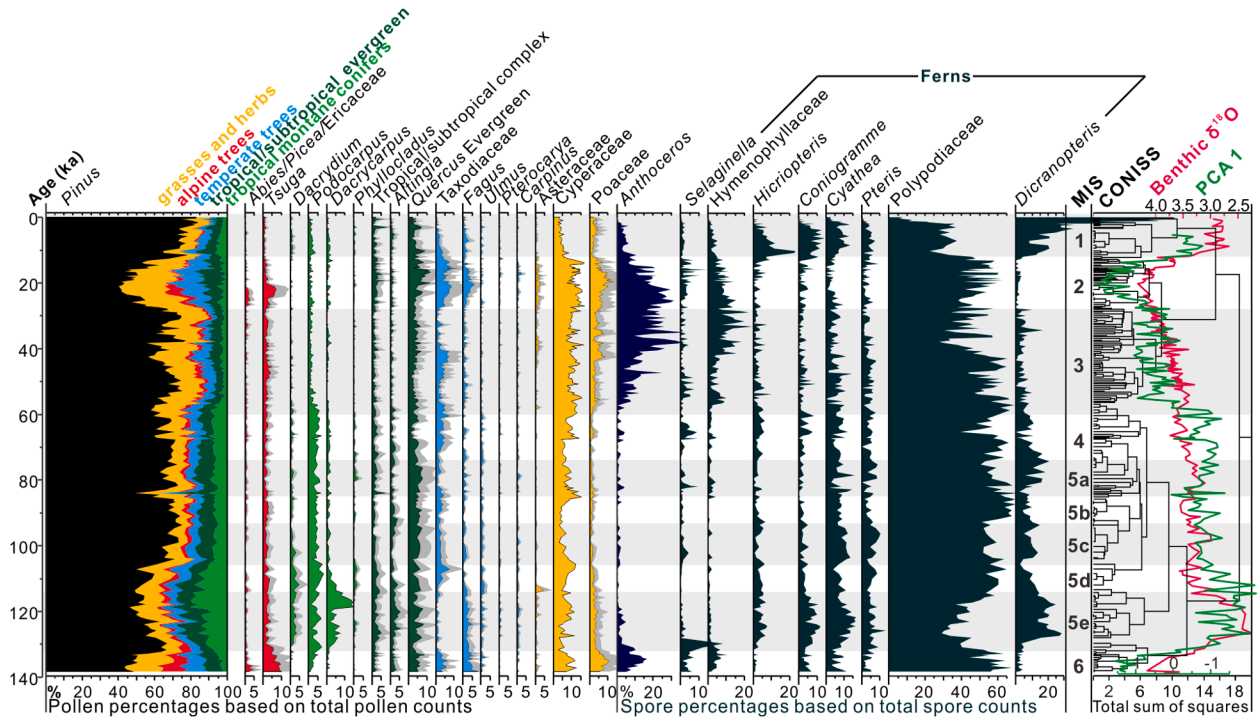


**Fig. 2.** Summary pollen diagram of core GeoB16602, showing percentages of ecological groups and major pollen and spore taxa, the cluster analysis (CONISS) dendrogram, benthic foraminiferal $\delta^{18}O$ curve and sample scores on PCA Axis1 (18.1% of total pollen variance, excluding Cyperaceae). Horizontal grey bars indicate the relatively warm marine isotope stages.

confirmed by the concentration (absolute abundance) data (Fig. S4). The successive peaks of Cyperaceae and *Selaginella* are commonly followed by a slight increase in *Pinus*, together forming a recurrent succession (Fig. 3E). The succession usually occurs at the transitions from cold to warm conditions, such as the glacial terminations, MIS 5d/5c, 5b/5a, 4/3 boundaries, the ends of Heinrich stadials and several Dansgaard-Oeschger (D/O) oscillations (Fig. 3).

## 5. Discussion

### 5.1. Pollen records offshore as indicators of coastal wetlands

Our pollen record from marine sedimentary archive corroborates surrounding terrestrial records (e.g. Zheng & Lei, 1999; Sheng et al., 2017; Wang et al., 2019), demonstrating clear glacial/interglacial shifts in the zonal tropical/subtropical vegetation of southern China. The abundance variations of Cyperaceae pollen, however, apparently differ from the long-term evolution of zonal forests, illustrating muted glacial cycle but persistent millennial-scale fluctuations (Figs. 2 and 3). More specifically, the short-term peaks of Cyperaceae at GeoB16602 mostly predate the relatively long-lasting interglacials or interstadials (such as MIS 5a, 5c, 5e and Greenland interstadials 1–18), of which a humid climate (Cheng et al., 2016; Fig. 3A) is often favorable for the expansion of inland freshwater wetlands (Bush, 2002). We also note that Cyperaceae pollen is quite common at most other sites of the East Asian Marginal seas during glacial periods (e.g. Zheng et al., 2013; Sun et al., 2003; Dai et al., 2015), as freshwater wetlands (anastomosing rivers, streams, bogs, and swamps) might be extensively developed on the exposed gently dipping continental shelves during sea-level lowstands, and shortened transportation distance facilitates the accumulation of Cyperaceae pollen (with relatively low dispersal ability, Dai et al., 2014; Yu et al., 2017) at offshore sites. In these cases, sea-level has a negative effect on Cyperaceae pollen abundances, their variations generally reflect glacial/interglacial cycles (Zheng et al., 2013; Sun et al., 2003), a distinctively different pattern from that exhibited by GeoB16602. All these contrasts strongly hint the weak correlation between GeoB16602 Cyperaceae pollen and regional climates, and probably limited contribution of freshwater wetlands to the short-term variations in Cyperaceae pollen abundance. Large amounts of alpine meadow origin Cyperaceae pollen can be excluded either, since other alpine species, such as *Abies/Picea* and Ericaceae, are nearly absent throughout our core (Fig. 2).

On the other hand, the recurrent Cyperaceae- *Selaginella*- *Pinus* succession at GeoB16602 closely mimics the Chenopodiaceae-Cyperaceae, Poaceae and mangroves- *Selaginella*-forests succession at MD03-2622 (González & Dupont, 2009), implying a universal ecological process that can be easily explained in the context of coastal saline environments. Initially, Chenopodiaceae species (e.g. *Salicornia*, *Atriplex* and *Suaeda*) occupy a hypersaline area. They are replaced by grasses (e.g. *Spartina* and *Sporobolus*), sedges (e.g. *Cyprus*, *Juncus* and *Scirpus*) and mangroves while soil salinity decreases to a moderate level. Forests are eventually established if soil conditions keep improving. Such plant communities are commonly found along world's seacoasts (Fig. S2). The absence of some phases in GeoB16602 succession can be attributed to biogeographic difference between two regions. Today Chenopodiaceae species are rarely found at the Pearl River estuary probably due to a more humid climate, since annual mean precipitation of southern China is nearly twice of northern Venezuela, and plenty rainfall may leach out excess salts and preclude the formation of hypersaline conditions. Poaceae species, such as *Spartina*, are not major components of salt marsh vegetation at the Pearl River estuary (Zhao, 1996). An overall glacial cycle for Poaceae pollen in our record (Fig. 2) also implies more climate-relevant evolution than Cyperaceae and a more likely regional provenance. Despite a sparse distribution of mangroves at today's Pearl River estuary (Zhao, 1996), its pollen is almost absent from surface sedimentary samples beyond the coastline (Dai et al., 2014; Yu et al., 2017). Mangrove pollen could become more undetectable at our site during glacial periods considering a southward shift of tropical/subtropical vegetation. By contrast, Cyperaceae, as the main component of modern salt marsh at the Pearl River estuary (Zhao, 1996), is much better expressed by pollen in modern offshore deposits, with a slight

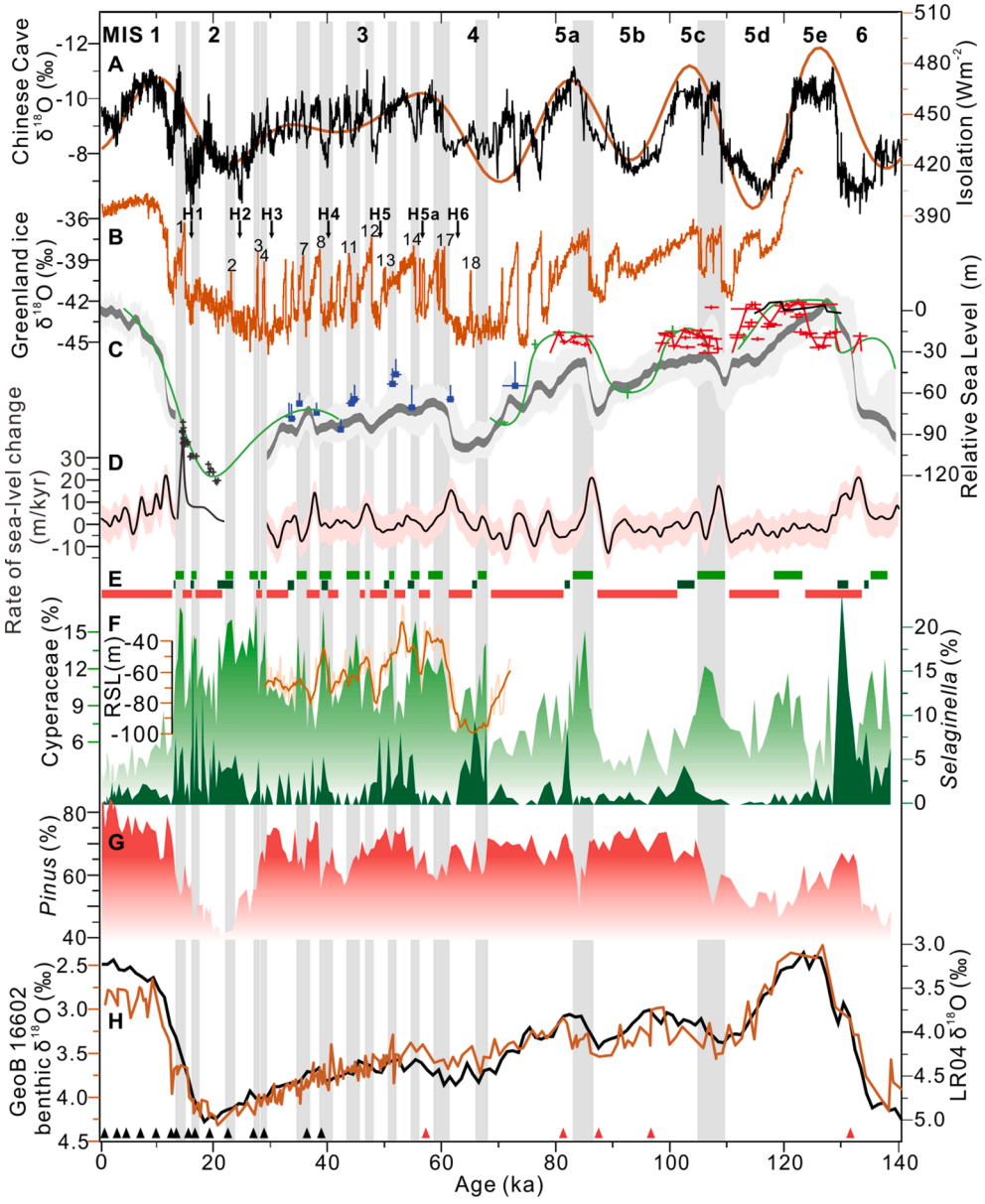


**Fig. 3.** Time series of coastal vegetation, sea level and climate records over the last glacial cycle. A: Composite Asian monsoon $\delta^{18}O$ record of Chinese stalagmites (Cheng et al., 2016) and 21 July insolation at 65°N. B: $\delta^{18}O$ record of Greenland Ice (North Greenland Ice Core Project (NGRIP) members, 2004). Arrows and numbers indicate possibly correlated millennial-scale climatic events. C: Sea-level reconstructions based on Red Sea planktic $\delta^{18}O$ (Grant et al., 2012), Sunda shelf sediments (black crosses, Hanebuth et al., 2000) and coral data (blue, green, and red, see references in Grant et al., 2012; black line, O'Leary et al., 2013). D: Rates of sea-level change calculated from Hanebuth et al. (2000) and Grant et al. (2012). E: Coastal wetland vegetation succession recorded in GeoB16602. Wetland herb (light green)-pioneer species (dark green, abundance recalculated excluding *Anthoceros* from the spore sum)-regional forest (pink) phases correspond to peak abundances of representative taxa in F and G. Sea level (RSL) reconstruction based on central Red Sea planktic $\delta^{18}O$ (light line) with 500 year moving average (heavy line) (Siddall et al., 2003) is superimposed on the Cyperaceae abundance record (F). H: Age control of GeoB16602 based on AMS $^{14}C$ dates (black triangles) and matching the benthic $\delta^{18}O$ curve with LR04 stack (Lisiecki & Raymo, 2005) (red triangles indicate the tie points). Vertical grey bars indicate wetland expansion events at the palaeo-Pearl River estuary. (For interpretation of the references to colour in this figure legend, the reader is referred to the web version of this article.)

decreasing trend in abundance (from > 10% to ~ 5–10%) from coastline to continental slope (Dai et al., 2014; Yu et al., 2017). Cyperaceae is therefore the most representative pollen type for coastal wetlands at site GeoB16602. An intriguing finding at both sites is the constantly repeated increases in *Selaginella*. Although it is difficult to find modern analogue for exact species in ecosystem shifts from saline water to land, the genus *Selaginella*, overall, prefers moist habitat and depends on water for fertilization (Banks, 2009; Setyawan et al., 2016). Its short-term blooms likely indicate the still moist soil condition at the early stage of forest establishment.

In brief, the temporal succession may help to identify some taxonomically inadequate palynomorphs (e.g. Cyperaceae and Poaceae) as salt marsh taxa (González & Dupont, 2009 and this study). Mangroves (e.g. Rhizophora and Sonneratia), in addition, are identified precisely by pollen (e.g. Grindrod et al., 1999; Scourse et al., 2005; Hendy et al., 2016). Pollen analysis of offshore deposits overall provide a powerful tool for the study of coastal wetland evolution during Quaternary sea-level changes.

### 5.2. Response of coastal wetland to Quaternary sea-level changes

The increases of Cyperaceae at GeoB16602 were closely linked to rapid sea-level rises over the past 140 kyr (Fig. 3). The increases of Cyperaceae at around 85 ka and 106 ka, for instance, coincide with sea-level rises at the MIS 5b/5a and MIS 5d/5c transitions (20–40 m, up to 22 m/kyr, Grant et al., 2012; Fig. 3D). The increase at around 120 ka might be related, within uncertainty, with the sea-level rise at the end of the last interglacial (9 m, 9 m/kyr, O'Leary et al., 2013). The latest and most remarkable increase, with an adequate chronological control, was well aligned with the MWP-1A (melt water pulse 1A) event (14–18 m, 40 m/kyr, Hanebuth et al., 2000; Fig. 3D and S5). The high-frequency variations of Cyperaceae abundance between 25 and 70 ka also seem to agree with the millennial-scale sea-level changes (Fig. 3F), given the ongoing debates on the timing of such sea-level fluctuations (Siddall et al., 2008; see Fig. 3C and F for the discrepancy among reconstructions) and our relatively rough chronology for this time interval. All the four (or five) major sea-level rises correlated to Heinrich events (H4-H6) or Antarctic events (A1-A4) (20–30 m, 8–16 m/kyr, Siddall et al., 2003; Arz et al., 2007; Fig. 3F), can find their counterparts

in the GeoB16602 Cypreaceae pulses. Pollen signature of even some lower-amplitude sea-level rises corresponding to D/O events 3, 4, 7, 11, 13, 18 (10–20 m, 5–10 m/kyr, Siddall et al., 2008; Fig. 3) is likely to be identified. Coeval rises of coastal wetland pollen abundance and sea-level are also found elsewhere worldwide, such as Sahul region (Grindrod et al., 1999), Congo fan (Scourse et al., 2005), Cariaco Basin (González & Dupont, 2009) and Gulf of Tehuantepec (Hendy et al., 2016).

Coastal wetland pollen abundance at offshore site is mainly determined by two aspects: distribution area of wetlands and transportation distance of their pollen. Since transportation distance increased during sea-level rises, exerting a negative effect on coastal wetland pollen (Zheng et al., 2013; Dai et al., 2014; Yu et al., 2017), it was thus more likely that coastal wetland vegetation expanded. A straightforward explanation is that the flat topographies, such as delta and floodplain, were flooded during rising sea-level, enlarging the shallow water bodies and distribution area of coastal wetland vegetation (Fig. 4A, B).

The following sharp decreases of Cyperaceae pollen demonstrate that such coastal wetlands might have rapidly shrunk into narrow bands while the sea level became relatively stable (Fig. 3D). The successive peaks of *Selaginella* spore and *Pinus* pollen suggest a colonization of zonal forest into those previously tidal-influenced areas. Subsequent gradual sea-level fall, for instances, during the mid-late parts of MIS 5a and 5c, would have exposed the flat topographies to fluvial incision and channel down-cutting. But new deltas and floodplains would prograde at the estuary when sea-level change decelerated, analogous to the mid-late Holocene processes of the large rivers draining into the SCS (Tanabe et al., 2006; Tamura et al., 2009; Zong et al., 2012), reserving a precondition for wetland expansion during the next sea-level rise (Fig. 4C).

Nevertheless, we notice that Cyperaceae peaks were absent during the latter part of each deglaciation at GeoB16602 (10–14 ka, 128–134 ka, Fig. 3F). A possible explanation is that too prolonged transport distance diluted coastal vegetation signals (Zheng et al., 2013; Chen et al., 2020). However, the sea-levels during these intervals were lower than MIS 5c-5e intervals where wetland expansions have been well documented (Fig. 3F). We propose that the flat topographies developed during the sea-level lowstands of MIS 2 and 6 (Fig. 4C) had been totally flooded by earlier deglaciation sea-level rises, leaving insufficient geomorphic conditions for the expansion of coastal wetlands during the following continuous sea-level rise of latter deglaciation. A lack of large rivers and limited delta platforms to host shallow waters in northeastern SCS coasts may also partly explain the much weak correlation between Cyperaceae pollen abundance and rapid sea-level rises during MIS 3 at a nearby site MD05-2906 (Dai et al., 2015).

### 5.3. *Implications for coastal wetland sustainability*

An important implication from our palaeoecological observation is that coastal wetlands may not only survive, but even expand during sea-level rises with rates up to 40 m/kyr (equal to mm/yr), contrary to the expected vulnerability based on Holocene coastal stratigraphic records of Great Britain (Horton et al., 2018) and Mississippi Delta (Törnqvist et al., 2020). A probable explanation to this discrepancy is the horizontal adaptability of coastal wetlands. Despite a widespread concern in both ecological and palaeoecological studies over the vertical adaptability of coastal wetlands (e.g. Morris et al., 2002; Craft et al., 2009; Nicholls & Cazenave, 2010; Fagherazzi et al., 2012; Horton et al., 2018; Törnqvist et al., 2020), it is recently hypothesized that landward migration into newly formed habitats may play a primary role in the survival of coastal wetlands through sea-level rise (Kirwan et al., 2016a; 2016b). A recent model considering the horizontal adaptability suggest that, albeit with widespread in place submergence, globally, coastal wetland will gain area under rapid sea-level rise scenario if sufficient accommodation space can be created through nature-based adaptation strategies (Schuerch et al., 2018). Our findings provide strong empirical evidence

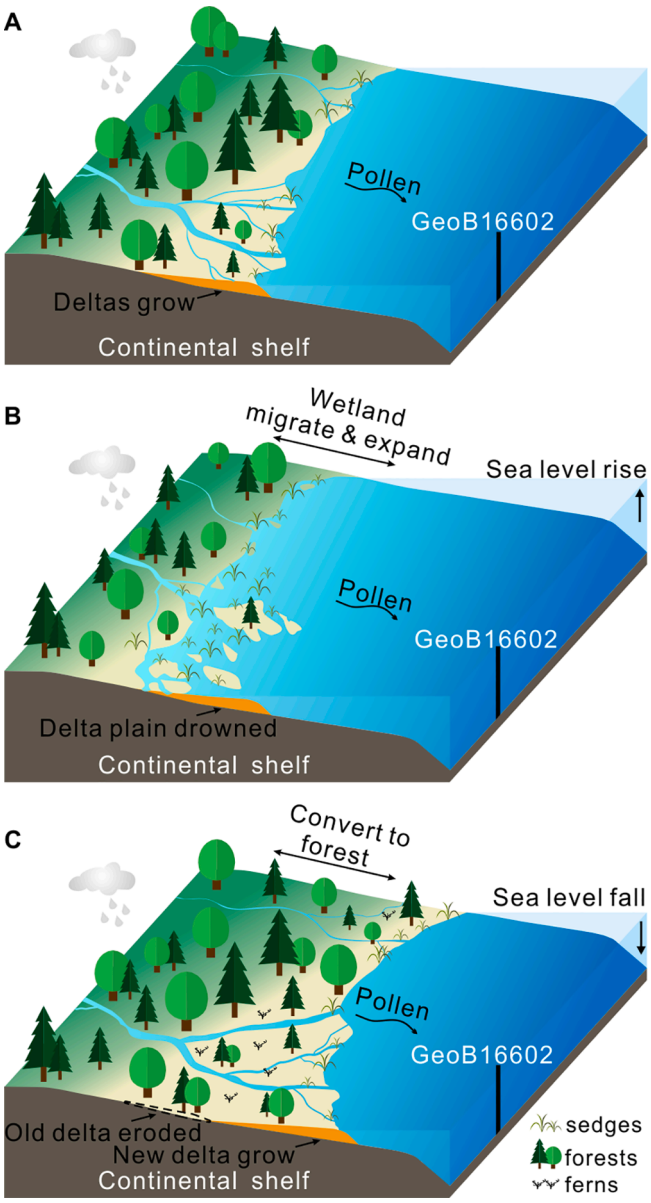


**Fig. 4.** Schematic diagram illustrating coastal wetland responses to sea level changes. A: Delta plains prograde when sea-level is relatively stable. Wetland vegetation are mainly distributed along the coastline. B: Coastal platforms are flooded by rising sea level, shallow water areas and consequently the wetland vegetation expand. Only migration happens at a steeper slope. C: Shallow water areas shrink during sea-level fall. Wetlands are replaced by zonal forest initiated with a pioneer fern occupation. If sea-level drops to lower than in A, former platforms are eroded, new delta plains prograde at the estuary when sea-level change decelerates.

for this prediction. Although it is hard to directly evaluate the vertical versus horizontal behaviors of coastal wetlands based on an offshore record, taking into account $>$ 20 m rises in sea-level during these centurial- or millennial-scale events and corresponding large-scale shoreline shifts on the gently dipping SCS continental shelf (Hanebuth et al., 2000; Wang et al., 2009), it is reasonable to suppose that *in-situ* persistence contributed little to the observed expansions of coastal wetlands. The regional (horizontal) behavior may not be explicitly reflected in Holocene coastal records (Horton et al., 2018; Törnqvist et al., 2020) due to limited spatial coverage of drilled cores and/or relatively low-amplitude sea-level changes.

Rather than the rates of sea-level rise, geomorphological settings will

probably be more decisive in the fate of coastal wetlands. Gently sloping uplands, such as large river delta plains, will favor the migration and even expansion of coastal wetlands (Fig. 4), whereas steep topography, including anthropogenic infrastructures, will lead to contraction or even local extinction of coastal wetlands with sea-level rise (Kirwan et al., 2016a; Kirwan et al., 2016b). Besides direct human modification, damming of rivers has been highlighted as a major threaten to coastal wetlands, because reduced sediment delivery not only restricts the vertical accretion rate and thus impedes the *in-situ* persistence (Kirwan & Megonigal, 2013; Lovelock et al., 2015), but also results in delta erosion (Syvitski et al., 2009) and eventually a reduction of lateral accommodation space. However, a recent study shows that not all deltas lose land area after damming; moreover, considering the contribution of deforestation-induced increase in sediment supply, human impact has led to net land area gain for global deltas over the past decades (Nienhuis et al., 2020), which might result in an overall improved geomorphic condition for the maintenance of coastal wetlands in the anthropogenic era.

## 6. Conclusions

The Geob16602 pollen record unveils two distinct evolution patterns of vegetation in southern China over the last 140 kyr. The zonal forest exhibited clear glacial-interglacial cycle while wetland vegetation showed prominent millennial-scale fluctuations. Replication of wetland-pioneer species-zonal forest succession from both South China Sea and Cariaco basin suggests that coastal wetland signals might be well distinguished in offshore sediments despite low taxonomic resolution of some key taxa (e.g. Cyperaceae) in pollen analysis. Salt marshes were found to have expanded at palaeo-Pearl River estuary during most episodes of rapid sea-level rise (10–40 m magnitudes, 8–40 m/kyr rates) over the last glacial cycle, indicating strong sustainability of coastal wetlands through historical sea-level change impacts. Coastal wetland systems can be well retained in face of future global sea-level rise if given sufficient accommodation space.

### *CRediT authorship contribution statement*

**Zhongjing Cheng:** Conceptualization, Data curation, Methodology, Writing – original draft. **Chengyu Weng:** Conceptualization, Methodology, Writing – review & editing. **Stephan Steinke:** Conceptualization, Resources, Writing – review & editing. **Mahyar Mohtadi:** Conceptualization, Resources, Writing – review & editing.

### Declaration of Competing Interest

The authors declare that they have no known competing financial interests or personal relationships that could have appeared to influence the work reported in this paper.

### *Acknowledgements*

We thank Dang HW, Ge HM, Wu JW, Liu JJ and Chen YR for their help in laboratory work. This work was supported by the NSFC (Grants: 42002026, 41877429, 91028010, and 91128211), China Postdoctoral Science Foundation (BX20190238 and 2020M671199) and the German BMBF (Grants: INVERS 03G0221A and CARIMA 03G0806B).

### *Data Availability Statement*

The pollen data used in this study will be submitted to PANGAEA (https://www.pangaea.de/),

## Appendix A. Supplementary data

Supplementary data to this article can be found online at https://doi.org/10.1016/j.ecolind.2021.108405.

## References

Aburto-Oropeza, O., Ezcurra, E., Danemann, G., Valdez, V., Murray, J., Sala, E., 2008. Mangroves in the Gulf of California increase fishery yields. Proc. Natl. Acad. Sci. USA 105 (30), 10456–10459.
Arz, H.W., Lamy, F., Ganopolski, A., et al., 2007. Dominant Northern Hemisphere climate control over millennial-scale glacial sea-level variability. Quat. Sci. Rev. 26, 312–321.
Banks, J.A., 2009. *Selaginella* and 400 million years of separation. Annu. Rev. Plant Biol. 60, 223–238.
Barnosky, A.D., Hadly, E.A., Gonzalez, P., et al., 2017. Merging palaeobiology with conservation biology to guide the future of terrestrial ecosystems. Science 355, eaab4787.
Beck, H.E., Zimmermann, N.E., McVicar, T.R., 2018. Present and future Köppen-Geiger climate classification maps at 1-km resolution. Sci. Data 5, 180214.
Brewer, S., Jackson, S.T., Williams, J.W., 2012. Palaeoecoinformatics: applying geohistorical data to ecological questions. Trends Eco. Evol. 27, 104–112.
Bush, M.B., 2002. On the interpretation of fossil Poaceae pollen in the lowland humid neotropics. Palaeogeogr. Palaeocl. Palaeoecol. 177, 5–17.
Chen, Y.R., Huang, E.Q., Schefuß, E., et al., 2020. Wetland expansion on the continental shelf of the northern South China Sea during sea level rise. Quat. Sci. Rev. 231, 106202.
Cheng, H., Edwards, R.L., Sinha, A., Spötl, C., Yi, L., Chen, S., Kelly, M., Kathayat, G., Wang, X., Li, X., Kong, X., Wang, Y., Ning, Y., Zhang, H., 2016. The Asian monsoon over the past 640,000 years and ice age terminations. Nature 534 (7609), 640–646.
Cheng, Z.J., Weng, C.Y., Steinke, S., Mohtadi, M., 2018. Anthropogenic modification of vegetated landscapes in southern China from 6,000 years ago. Nat. Geosci. 11, 939–943.
Church, J.A., Clark, P.U., Cazenave, A., et al., 2013. Sea Level Change. In: Stocker, T.F., Qin, D., Plattner, G.K. (Eds.), Climate Change 2013: The Physical Science Basis. Cambridge University Press, Cambridge.
Craft, C., Clough, J., Ehman, J., et al., 2009. Forecasting the effects of accelerated sea-level rise on tidal marsh ecosystem services. Front. Ecol. Environ. 7, 73–78.
Dai, L.u., Weng, C., Lu, J., Mao, L., 2014. Pollen quantitative distribution in marine and fluvial surface sediments from the northern South China Sea: New insights into pollen transportation and deposition mechanisms. Quatern. Int. 325, 136–149.
Dai, L., Weng, C.Y., Mao, L.M., 2015. Patterns of vegetation and climate change in the northern South China Sea during the last glaciation inferred from marine palynological records. Palaeogeogr. Palaeocl. Palaeoecol. 440, 249–258.
Duarte, C.M., Losada, I.J., Hendriks, I.E., Mazarrasa, I., Marba, N., 2013. The role of coastal plant communities for climate change mitigation and adaptation. Nat. Clim. Change 3, 961–968.
Fagherazzi, S., Kirwan, M.L., Mudd, S.M., Guntenspergen, G.R., Temmerman, S., D'Alpaos, A., van de Koppel, J., Rybczyk, J.M., Reyes, E., Craft, C., Clough, J., 2012. Numerical models of salt marsh evolution: Ecological, geomorphic, and climatic factors. Rev. Geophys. 50 (1) https://doi.org/10.1029/2011RG000359.
Fægri, K., Kaland, P.E., Krzywinski, K., 1989. Textbook of Pollen Analysis. Wiley, New York.
González, C., Dupont, L.M., 2009. Tropical salt marsh succession as sea-level indicator during Heinrich events. Quat. Sci. Rev. 28.
Grant, K.M., Rohling, E.J., Bar-Matthews, M., et al., 2012. Rapid coupling between ice volume and polar temperature over the past 150,000 years. Nature 491, 744–747.
Grimm, E.C., 1987. CONISS: a Fortran 77 program for stratigraphically constrained cluster analysis by the method of the incremental sum of squares: *Comp*. Geosci. 13, 13–35.
Grindrod, J., Moss, P., Kaars, S.V.D., 1999. Late Quaternary cycles of mangrove development and decline on the north Australian continental shelf. J. Quaternary Sci. 14 (5), 465–470.
Hanebuth, T., Stattegger, K., Grootes, P.M., 2000. Rapid flooding of the Sunda shelf: a late-glacial sea-level record. Science 288 (5468), 1033–1035.
Hendy, I.L., Minckley, T.A., Whitlock, C., 2016. Eastern tropical Pacific vegetation response to rapid climate change and sea level rise: A new pollen record from the Gulf of Tehuantepec, southern Mexico. Quat. Sci. Rev. 145, 152–160.
Horton, B.P., Shennan, I., Bradley, S.L., Cahill, N., Kirwan, M., Kopp, R.E., Shaw, T.A., 2018. Predicting marsh vulnerability to sea-level rise using Holocene relative sea-level data. Nat. Commun. 9 (1) https://doi.org/10.1038/s41467-018-05080-0.
International Atomic Energy Agency Global Network of Isotopes in Precipitation (GNIP): the GNIP database 2013 http://www-naweb.iaea.org/napc/ih/IHS_resources_gnip.html.
Kirwan, M.L., Guntenspergen, G.R., D'Alpaos, A., Morris, J.T., Mudd, S.M., Temmerman, S., 2010. Limits on the adaptability of coastal marshes to rising sea level. Geophys. Res. Lett. 37 (23), n/a–n/a.
Kirwan, M.L., Megonigal, J.P., 2013. Tidal wetland stability in the face of human impacts and sea-level rise. Nature 504 (7478), 53–60.
Kirwan, M.L., Temmerman, S., Skeehan, E.E., Guntenspergen, G.R., Fagherazzi, S., 2016a. Overestimation of marsh vulnerability to sea level rise. Nat. Clim. Change 6 (3), 253–260.
Kirwan, M.L., Walters, D.C., Reay, W.G., Carr, J.A., 2016b. Sea level driven marsh expansion in a coupled model of marsh erosion and migration. Geophys. Res. Lett. 43 (9), 4366–4373.
Lisiecki, L.E., Raymo, M.E., 2005. A Pliocene-Pleistocene stack of 57 globally distributed benthic delta O-18 records. Palaeoceanography 20, PA1003.

Liu, J.G., Steinke, S., Vogt, C., et al., 2017. Temporal and spatial patterns of sediment deposition in the northern South China Sea over the last 50,000 years. Palaeogeogr. Palaeoclimat. Palaeoecol. 465, 212–224.
Lovelock, C.E., Cahoon, D.R., Friess, D.A., Guntenspergen, G.R., Krauss, K.W., Reef, R., Rogers, K., Saunders, M.L., Sidik, F., Swales, A., Saintilan, N., Thuyen, L.X., Triet, T., 2015. The vulnerability of Indo-Pacific mangrove forests to sea-level rise. Nature 526 (7574), 559–563.
Millennium Ecosystem Assessment, 2005. Ecosystems and Human Well-Being: Biodiversity Synthesis. World Resources Institute, Washington, DC.
Mohtadi, M. and cruise participants. (2012) Report and preliminary results of RV Sonne cruise SO 221. INVERS. Hongkong-Hongkong, 17.05.2012-07.06.2012. *Berichte Fachbereich Geowissenschaften Universität Bremen*, 288, 168.
Morris, J.T., Sundareshwar, P.V., Nietch, C.T., Kjerfve, B., Cahoon, D.R., 2002. Responses of coastal wetlands to rising sea level. Ecology 83 (10), 2869–2877.
Möller, I., Kudella, M., Rupprecht, F., et al., 2014. Wave attenuation over coastal salt marshes under storm surge conditions. Nat. Geosci. 7, 727–731.
North Greenland Ice Core Project (NGRIP) members, 2004. High-resolution record of Northern Hemisphere climate extending into the last interglacial period. Nature 431, 147–151.
Nicholls, R.J., Wong, P.P., Burkett, V.R., et al., 2007. Coastal systems and low-lying areas. In: Parry, M.L. (Ed.), Climate Change 2007: Impacts, Adaption and Vulnerability. Contribution of Working Group II to the Fourth Assessment Report of the Intergovernmental Panel on Climate Change. Cambridge University Press, Cambrige, pp. 315–356.
Nicholls, R.J., Cazenave, A., 2010. Sea-level rise and its impacts on coastal zones. Science 328, 1517–1520.
Nienhuis, J.H., Ashton, A.D., Edmonds, D.A., Hoitink, A.J.F., Kettner, A.J., Rowland, J. C., Törnqvist, T.E., 2020. Global-scale human impact on delta morphology has led to net land area gain. Nature 577 (7791), 514–518.
O'Leary, M.J., Hearty, P.J., Thompson, W.G., et al., 2013. Ice sheet collapse following a prolonged period of stable sea level during the last interglacial. Nat. Geosci. 6, 796–800.
Paillard, D., Labeyrie, L., Yiou, P., 1996. Macintosh program performs time-series analysis. Eos Transactions American Geophysical Union 77 (39), 379.
Parkinson, R.W., Harlem, P.W., Meeder, J.F., 2015. Managing the Anthropocene marine transgression to the year 2100 and beyond in the State of Florida U.S.A. Climatic Change 128 (1-2), 85–98.
Parkinson, R.W., Craft, C., DeLaune, R.D., et al., 2016. Marsh vulnerability to sea-level rise. Nat. Clim. Change 7, 756.
Rogers, K., Kelleway, J.J., Saintilan, N., Megonigal, J.P., Adams, J.B., Holmquist, J.R., Lu, M., Schile-Beers, L., Zawadzki, A., Mazumder, D., Woodroffe, C.D., 2019. Wetland carbon storage controlled by millennial-scale variation in relative sea-level rise. Nature 567 (7746), 91–95.
Schuerch, M., Spencer, T., Temmerman, S., Kirwan, M.L., Wolff, C., Lincke, D., McOwen, C.J., Pickering, M.D., Reef, R., Vafeidis, A.T., Hinkel, J., Nicholls, R.J., Brown, S., 2018. Future response of global coastal wetlands to sea-level rise. Nature 561 (7722), 231–234.
Scourse, J., Marret, F., Versteegh, G.J.M., Jansen, J.H.F., Schefuß, E., van der Plicht, J., 2005. High-resolution last deglaciation record from the Congo fan reveals significance of mangrove pollen and biomarkers as indicators of shelf transgression. Quaternary Res. 64 (1), 57–69.
Sheng, M., Wang, X.S., Zhang, S.Q., et al., 2017. A 20,000-year high-resolution pollen record from Huguangyan Maar Lake in tropical-subtropical South China. Palaeogeogr. Palaeoclimatol. Palaeoecol. 472, 83–92.
Siddall, M., Rohling, E.J., Almogi-Labin, A., Hemleben, C.h., Meischner, D., Schmelzer, I., Smeed, D.A., 2003. Sea-level fluctuations during the last glacial cycle. Nature 423 (6942), 853–858.
Siddall, M., Rohling, E.J., Thompson, W.G., Waelbroeck, C., 2008. Marine isotope stage 3 sea level fluctuations: Data synthesis and new outlook. Rev. Geophys. 46, RG4003.
Setyawan, A.D., Supriatna, J., Darnaedi, D., et al., 2016. Diversity of Selaginella across altitudinal gradient of the tropical region. Biodiversitas 17, 384–400.
Sun, X., Luo, Y., Huang, F., Tian, J., Wang, P., 2003. Deep sea pollen from the South China Sea: Pleistocene indicators of East Asian monsoon. Mar. Geol. 201 (1-3), 97–118.
Syvitski, J.P.M., Kettner, A.J., Overeem, I., et al., 2009. Sinking deltas due to human activities. Nat. Geosci. 2, 681–686.
Tamura, T., Saito, Y., Sieng, S., Ben, B., Kong, M., Sim, I.m., Choup, S., Akiba, F., 2009. Initiation of the Mekong River delta at 8 ka: evidence from the sedimentary succession in the Cambodian lowland. Quat. Sci. Rev. 28 (3-4), 327–344.
Tanabe, S., Saito, Y., Vu, Q.L., et al., 2006. Holocene evolution of the Song Hong (Red River) delta system, northern Vietnam. Sediment. Geol. 187, 29–61.
ter Braak, C.J.F., Smilauer, P., 1998. CANOCO reference manual and user's guide to CANOCO for windows, 4th ed. Center for biometry, Wageningen, New York.
Törnqvist, T.E., Jankowski, K.L., Li, Y.X., González, J.L., 2020. Tipping points of Mississippi Delta marshes due to accelerated sea-level rise. Sci. Adv. 6, eaaz5512.
Wang, X.M., Sun, X.J., Wang, P.X., Stattegger, K., 2009. Vegetation on the Sunda Shelf, South China Sea, during the Last Glacial Maximum. Palaeogeogr. Palaeoclimatol. Palaeoecol. 278, 88–97.
Wang, W.M., Li, C.H., Shu, J.W., Chen, W., 2019. Changes of vegetation in southern China. Sci. China Earth Sci. 62, 1316–1328.
Wu, Z.Y., 1980. Vegetation of China. Science Press, Beijing, pp. 823–896.
Yu, S.H., Zheng, Z., Chen, F., et al., 2017. A last glacial and deglacial pollen record from the northern South China Sea: New insight into coastal-shelf palaeoenvironment. Quat. Sci. Rev. 157, 114–128.
Zhao, D.C., 1996. Coastal vegetation of China. China Ocean Press, Beijing, pp. 136–156.
Zheng, Z., Lei, Z.Q., 1999. A 400,000 year record of vegetation and climate change from a volcanic basin, Leizhou Peninsula, Southern China. Palaeogeogr. Palaeoclimatol. Palaeoecol. 145, 339–362.
Zheng, Z., Huang, K.Y., Deng, Y., et al., 2013. A ~200 ka pollen record from Okinawa Trough: Palaeoenvironment reconstruction of glacial-interglacial cycles. Sci. China Earth Sci. 56, 1731–1747.
Zong, Y., Huang, K., Yu, F., Zheng, Z., Switzer, A., Huang, G., Wang, N., Tang, M., 2012. The role of sea-level rise, monsoonal discharge and the palaeo-landscape in the early Holocene evolution of the Pearl River delta, southern China. Quat. Sci. Rev. 54, 77–88.